DETECTION AND CHARACTERIZATION OF IONOSPHERIC ACTIVITY AT HIGH LATITUDE FROM SAR MEASUREMENTS

Aymeric Mainvis, Vincent Fabbro

ONERA / DEMR, Université de Toulouse, F-31055 Toulouse - France

ABSTRACT

This paper describes a methodology to detect and characterize the ionospheric activity thanks to spaceborne synthetic aperture radar (SAR) measurements. This strategy is based on the Faraday rotation (FR) estimation which leads to the Total Electron Content (TEC) quantification and the ionospheric phase advance assessment. The metrics are derived from these two previous quantities by using the mean value of the phase advance and the Rate of TEC Index. Both quantities are estimated along the azimuth path of the platform, where the ionosphere drastically disturbs the image synthesis. To perform the process, a fully-polarimetric SAR measurement is needed. The methodology is tested on different PALSAR acquisitions. A first case allows studying the ionospheric activity near Fairbanks, Alaska and a second one shows the occurrence of ionospheric disturbance during measurements over Greenland. The parameters succeed in detecting the ionospheric activity from a single SAR measurement. Then, the results are compared with GNSS measurements from the high-rate IGS network processed by the GAGE methodology. This shows that all scales in the ionosphere are interrelated, leading to an ionospheric scintillation event at the same time as the appearance of a TEC gradient. Simultaneous observation of the ionosphere by different means appears necessary to better understand the dynamics of this atmospheric layer.

Index Terms— Ionosphere, radio propagation, synthetic aperture radar (SAR)

1. INTRODUCTION

Low-frequency space-based SAR systems can be used for global surveillance. This mission is dedicated to the precise observation of local changes due to global climate change. In particular, they can measure the evolution of terrestrial biomass in equatorial regions and the decrease of ice fields in high latitude regions.

However, it is well known that, at these lower frequencies (L-band or below), the radar signal is affected by propagation through the ionospheric layer. The ionospheric background induces refraction, polarization rotation, group delay and phase advance mainly due to the large-scale variations of the electron content within the ionosphere. Also, the small-scale ionospheric structures generated by plasma instability processes affect the radar signal by adding a scattering phenomenon during the measurement, this is the ionospheric scintillation. These signal fluctuations reduce the quality of a SAR image, which may even prevent InSAR processing and change detection. Essentially, these disturbances occur in two regions, namely the polar cap and equatorial zones. More precisely, in the polar cap, ionospheric activity is more intense in the auroral oval. This location is an energy zone with a high electron density. For equatorial regions, the radar signal is frequently disturbed during the post-sunset periods because of electric fields resulting from the interaction of charged particles from the Sun, the geomagnetic field and the particle winds developed within the ionosphere.

The observation of ionospheric activity from SAR data has been an active subject for several years. In equatorial regions, this activity induces the occurrence of stripes aligned with the geomagnetic field. These patterns provide clues about the geometrical structure of the ionospheric irregularity, its altitude and its drift velocity [1] and some modelings succeed in retrieving similar shapes [2]. Also, thanks to fully polarimetric SAR data, FR can be estimated [3]. This effect is used to estimate TEC and to produce TEC map from SAR acquisitions [4]. Furthermore, the ionospheric scintillation parameter S_4 is estimated using two SAR acquisitions on two different dates [5] in India. The estimated S_4 is compared with the one measured by GNSS receivers positioned along the orbit of the space-borne SAR sensor and the results are qualitatively consistent. Moreover, an experiment was done to estimate the ionospheric scintillation effects in equatorial regions thanks to the measurement of the point spread function [6]. Here, the capability of SAR in quantitatively measuring an ionospheric parameter has been demonstrated by using a specific dedicated ground system.

In this study, two parameters are defined to detect and

The authors would like to thank JAXA and F. Meyer of the University of Alaska at Fairbanks, AK, USA, for providing the ALOS PALSAR data and Guillermo González-Casado of the Universitat Politecnica de Catalunya at Barcelona, Spain for the GNSS measurements. The research presented in this document is part of a contract funded by the European Space Agency (ESA 4000120868-17-NL-AF-hh). The authors would like to thank all those who participated in this project and especially Raul Orus Perez from ESA for supporting this work.

characterize the ionospheric activity at high latitude. They are derived from FR estimates thanks to fully polarimetric SAR data. These quantities are tested on quad-pol SAR data acquired by ALOS PALSAR over Fairbanks, Alaska and Greenland. The estimates are compared with GNSS measurements to assess the different scales impacted by the ionosphere during an episode of disturbances.

2. IONOSPHERIC ACTIVITY FROM SAR DATA

The space-time ionosphere variability introduces phase variations in range and azimuth directions and FR corrupting the polarimetric channels during the wave propagation path. Usually, TEC characterizing the ionosphere layer, is defined along a vertical path ($\mathrm{TEC_V}$). But for space borne SAR, TEC is defined along the propagation path from the SAR sensor to the given resolution cell located on the ground. Then, Slant TEC along the path is $TEC = \frac{TEC_V}{\cos\theta}$, where θ is the incidence angle at the effective altitude of the ionospheric layer. The relation between FR Ω and TEC is given by [3]

$$\Omega = \frac{\zeta e \mathbf{B}\cdot\hat{\kappa}}{c_0 m_e f^2} TEC, \tag{1}$$

where $\zeta = e^2/\left(8\pi^2\varepsilon_0 m_e\right) = 40.3082\ \mathrm{m^3/s^2}$, $\mathbf{B}$ is the geomagnetic field, $\hat{\kappa}$ is the unit wave propagation vector, c_0 is the speed of light, m_e is the mass of the electron, f is the EM frequency, e is the charge of the electron and ε_0 is the free-space permittivity. This expression can be easily applied at high latitudes but remains ineffective in equatorial regions because of near-zero values of $\mathbf{B}$ near the geomagnetic equator.
Here, FR is derived from the Bickel and Bates estimator [7] requiring fully-polarized SAR data given by the ALOS PALSAR sensor and, in a climatological context, the estimation of FR is a chance to directly monitor the ionosphere activity.

The phase advance φ introduced by the ionospheric layer during the two-way propagation path is [3]

$$\varphi = 2 \times \frac{2\pi\zeta}{c_0 f} TEC, \tag{2}$$

where a perfect correlation on the up and down paths is assumed. The main consequence is that the phase advance modifies the time-Doppler history of the received pulses and this phenomenon causes defocusing, geometric distortions and loss of interferometric coherence. By assuming a linear TEC gradient along the azimuth $\frac{\partial TEC}{\partial x}$, a given scatterer is then focused at a shifted position δa given by [3]

$$\delta a = 2\zeta v \frac{v_{\mathrm{piercing}}}{c_0 f D_f} \frac{\partial TEC}{\partial x}, \tag{3}$$

where v is the velocity of the platform, $v_{\mathrm{piercing}} = v \cdot h_{\mathrm{iono}}/h_{\mathrm{plat}}$ is the velocity of the piercing point at the ionospheric layer, h_{iono} is the altitude of the ionospheric layer, h_{plat} is the altitude of the platform and D_f is the Doppler rate. This leads to a loss of coherence in the interferogram between two co-located acquisitions.

Therewith, the common metrics used to monitor and characterize the ionospheric activity in the GNSS context can be applied in the SAR case by estimating the ionospheric phase screen from the TEC map (2) thanks to the estimated FR (1). Then, the standard deviation of the phase σ_φ can be derived to detect the ionospheric activity. A second indicator can be obtained, the Rate of TEC Index (ROTI) [8], which is the standard deviation of the Rate of TEC ($ROT = \frac{\partial TEC}{\partial t}$) in TECU/min. Here, from (3), ROTI is directly linked to the standard deviation of the shifted position in a given disturbed acquisition since $v_{\mathrm{piercing}}\frac{\partial TEC}{\partial x} = \frac{\partial x}{\partial t}\cdot\frac{\partial TEC}{\partial x} = \frac{\partial TEC}{\partial t}$ [3]. However, from a given TEC map, a spatial expression of ROTI along the azimuth is more relevant. This quantity, noted $ROTI_s$, is defined as $ROTI_s := \frac{ROTI}{v_{\mathrm{piercing}}}$ in TECU/km.

3. RESULTS AND DISCUSSION

The first case considers two acquisitions of the same location near Fairbanks, Alaska. One is disturbed by the ionospheric activity (ALPSRP063051300) on April 1st 2007 while the other is not (ALPSRP069761300) on May 17th 2007. FR is retrieved from the fully-polarized SLC (single look complex) data and the estimates are averaged over a window of 1 x 1 km^2 (i.e. about 32000 looks are averaged). It has to be highlighted that the FR is directly estimated from the focused SLC. Lavalle *et al.* [9] have shown that the FR estimated from PALSAR products reveals small differences between raw data and SLC data estimation if rapid spatial variations of TEC do not occur in the ionosphere. Here, the previous condition is achieved since a spatial averaging is done and so the rapid spatial variations of TEC are vanished. Moreover, it has been verified that the FR estimates are in agreement with those retrieved by Kim *et al.* [3] from the unfocused data. The FR map is then transformed into the phase advance map and the standard deviation of the phase and the $ROTI_s$ are estimated along the azimuth (Fig. 1). This result is consistent with the high ionospheric activity which induces an increasing of the phase advance fluctuation during the acquisition and so an increasing of σ_φ up to 33 rad. With the calmer ionospheric conditions, σ_φ remains very close to 5 rad.

The second scenario considers 91 acquisitions over Greenland on April 1st 2007 from 00:51 to 00:58 UTC. By applying the same data processing, the mean σ_φ along the azimuth of each acquisition is computed. These estimations are shown in Fig. 2 where σ_φ varies from 3 up to 18 rad. The red circle highlights a high ionospheric disturbance during the acquisitions ALPSRP063011270 and ALPSRP063011280 while the yellow one is a corrupted acquisition (ALPSRP063011220). In the two acquisitions impacted by the ionosphere, the estimated σ_φ are significant with values greater than 5 rad and reaching 17 rad, which is an evidence of the ionospheric activity.

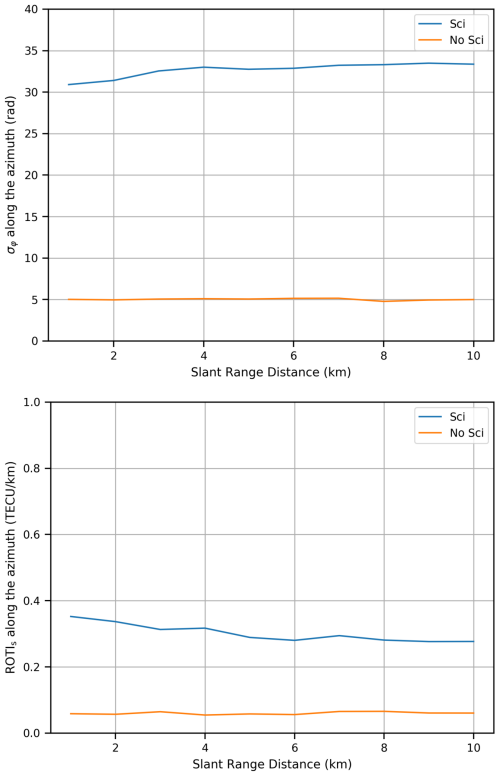

Fig. 1. Standard deviation of the phase advance (top) and $ROTI_s$ (down) along the azimuth. In blue color (Sci) during the high ionospheric activity and in orange (No Sci) with a calm ionosphere.

The identified TEC gradients from SAR data are a sign of ionospheric activity at a large spatial scale. However, during these ionospheric episodes, all the scales of the ionospheric layers are affected and the turbulence occurs from large to small spatial scales. This is confirmed by the scintillation parameters derived from GNSS measurements provided by the high-rate IGS network and presented in the following section.

4. MEASUREMENTS OF IONOSPHERIC SCINTILLATION: HIGH-RATE IGS NETWORK

The two GNSS stations analyzed here are the "kely" and "fair" stations located in Greenland and in Fairbanks, Alaska, respectively. The scintillation parameters are derived thanks to the GAGE processing [10, 11] which accurately detrends the carrier phase signals from GNSS satellites. The detrending of the satellite signals removes the satellite orbit and troposphere components, the carrier phase ambiguity and the clocks from both satellite and receiver, using the precise position of the receiver to leave only the ionosphere delay in the signals, from which the standard deviation of signal phase (σ_φ) is calculated. The derivation of STEC also allows to

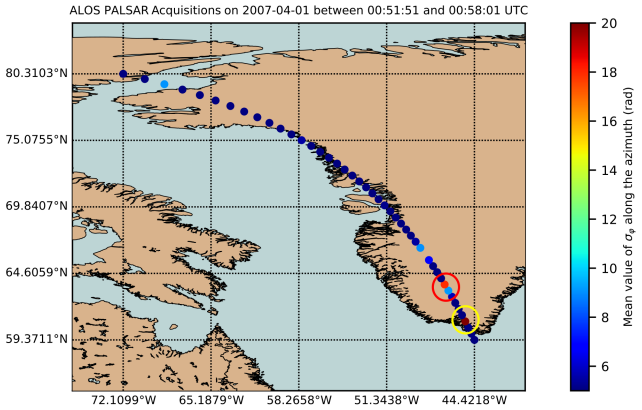

Fig. 2. Mean value of σ_φ along the azimuth during the flight over Greenland on April 1st UTC. The red circle is an ionospheric disturbance event, the yellow one is a corrupted acquisition.

correct the ionospheric delay in single carrier phase signals, allowing the calculation of a ROTI for individual signals. σ_φ, S_4 and ROTI are calculated for each satellite in view from a given receiver performing the average over a 60-seconds interval. No moving time window is applied in the calculations, so the parameters are provided at intervals of 1 minute after averaging values over the previous 60 seconds. The ROTI map measured by the station "fair" on April 1st 2007 between 07:00 and 08:00 UTC near Fairbanks, Alaska is plotted on the upper part of Fig. 3. The measured ROTI values range between 0 and about 3 TECU/min corresponding to a high ionospheric activity. Moreover, some high values of ROTI are measured in the direct neighborhood of the SAR acquisition, supporting the claim that ionosphere activity is causing the observed disturbance to the SAR data. The ROTI map measured by the station "kely" on April 1st 2007 between 00:00 and 02:00 UTC in Greenland is plotted on the lower part of Fig. 3. The measured ROTI values range between 0 and about 2.5 TECU/min corresponding to a high ionospheric activity. Moreover, some high values of ROTI are also measured near the SAR acquisition (northwest of the location). Then, the TEC gradient observed in the SAR data is certainly due to the ionospheric activity in this region at this moment.

5. CONCLUSION

Two parameters assessing the ionospheric activity from SAR acquisition have been defined. The first is the mean value of the phase advance along the azimuth. The second is the Rate of TEC Index along the azimuth in its spatial form, $ROTI_s$ in TECU/km. This parameter gives the spatial evolution of the electron content along the azimuth. These indicators have been tested on two different scenarios thanks to fully-

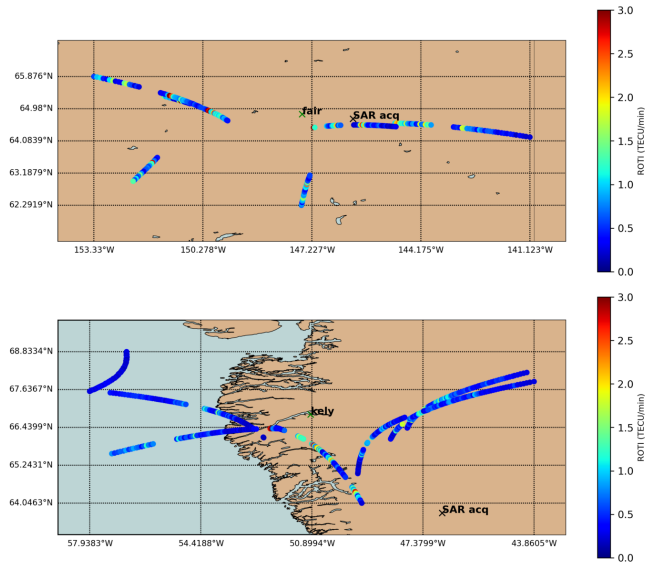

Fig. 3. Measured ROTI map on April 1st 2007, top: "fair" station between 07:00 and 08:00 UTC near Fairbanks, Alaska, down: "kely" station between 00:00 and 02:00 UTC in Greenland. The geographical location of each ROTI value is given by the ionospheric piercing point at an altitude of 200 km. The green cross is the location of the GNSS station and the black cross is the location of the PALSAR acquisition at 07:28 UTC (top) and 00:53 UTC (down).

polarimetric PALSAR acquisitions. The first case is focused on a well-known event with two acquisitions near Fairbanks, Alaska. The second one is a new identified event. It studies several acquisitions over Greenland. In both cases, both parameters manage to identify the ionospheric event. These phenomena are confirmed by the GNSS measurements provided by the high-rate IGS network showing an ionospheric scintillation event at the time of the SAR acquisitions. Also, the observation by two different means (SAR and GNSS) measuring different scales reveals that all scales of the ionosphere are impacted. Then, using several ionospheric observation tools is a relevant way to deeper study the ionosphere inhomogeneities and their dynamics.

Additional work is needed to test the suggested parameters on more disturbed SAR acquisitions and a new approach has to be defined to study the ionospheric activity in equatorial regions from a single SAR acquisition.

6. REFERENCES

[1] Jun Su Kim, Konstantinos P. Papathanassiou, Hiroatsu Sato, and Shaun Quegan, "Detection and Estimation of Equatorial Spread F Scintillations Using Synthetic Aperture Radar," *IEEE Trans. Geosci. Remote Sens.*, vol. 55, no. 12, pp. 6713–6725, dec 2017.

[2] Franz J. Meyer, Kancham Chotoo, Susan D. Chotoo, Barton D. Huxtable, and Charles S. Carrano, "The Influence of Equatorial Scintillation on L-Band SAR Image Quality and Phase," *IEEE Trans. Geosci. Remote Sens.*, vol. 54, no. 2, pp. 869–880, feb 2016.

[3] Jun Su Kim, Konstantinos P. Papathanassiou, Rolf Scheiber, and Shaun Quegan, "Correcting Distortion of Polarimetric SAR Data Induced by Ionospheric Scintillation," *IEEE Trans. Geosci. Remote Sens.*, vol. 53, no. 12, pp. 6319–6335, 2015.

[4] Franz Meyer and Jeremy Nicoll, "Mapping Ionospheric TEC using Faraday Rotation in Full- Polarimetric L-Band SAR Data," *Synth. Aperture Radar (EUSAR), 2008 7th Eur. Conf.*, pp. 1–4, 2008.

[5] S. Mohanty, G. Singh, C. S. Carrano, and S. Sripathi, "Ionospheric Scintillation Observation Using Space-Borne Synthetic Aperture Radar Data," *Radio Sci.*, vol. 53, pp. 1–16, 2018.

[6] D. P. Belcher, P. S. Cannon, and A. Gustavsson, "The ascension island experiment: Measurement of ionospheric scintillation effects on PALSAR-2," in *2015 IEEE Int. Geosci. Remote Sens. Symp.* jul 2015, pp. 3191–3194, IEEE.

[7] S. H. Bickel and R. H.T. Bates, "Effects of Magneto-Ionic Propagation on the Polarization Scattering Matrix," *Proc. IEEE*, vol. 53, no. 8, pp. 1089–1091, 1965.

[8] Iurii Cherniak, Andrzej Krankowski, and Irina Zakharenkova, "ROTI Maps: a new IGS ionospheric product characterizing the ionospheric irregularities occurrence," *GPS Solut.*, vol. 22, no. 3, jul 2018.

[9] Marco Lavalle, E Pottier, D Solimini, and N Miranda, "Faraday rotation estimation from unfocussed raw data: Analysis using ALOS PALSAR data," in *4th Int. Work. Sci. Appl. SAR Polarim. Polarim. Interferom. – PolInSAR 2009*, Frascati, Italy, 2009.

[10] J. M. Juan, A. Aragon-Angel, J. Sanz, G. González-Casado, and A. Rovira-Garcia, "A method for scintillation characterization using geodetic receivers operating at 1 Hz," *J. Geod.*, vol. 91, no. 11, pp. 1383–1397, nov 2017.

[11] Viet Khoi Nguyen, Adria Rovira-Garcia, José Miguel Juan, Jaume Sanz, Guillermo González-Casado, The Vinh La, and Tung Hai Ta, "Measuring phase scintillation at different frequencies with conventional GNSS receivers operating at 1 Hz," *J. Geod.*, vol. 93, no. 10, pp. 1985–2001, oct 2019.